

# In-situ X-ray absorption studies of bromine on the Ag(100) electrode<sup>☆</sup>

Osamu Endo <sup>a</sup>, Manabu Kiguchi <sup>a</sup>, Toshihiko Yokoyama <sup>a</sup>, Masatoshi Ito <sup>b</sup>,  
Toshiaki Ohta <sup>a,\*</sup>

<sup>a</sup> Department of Chemistry, Graduate School of Science, The University of Tokyo 7-3-1, Hongo, Bunkyo-ku, Tokyo 113-0033, Japan

<sup>b</sup> Department of Chemistry, Faculty of Science and Technology, Keio University, 3-14-1 Hiyoshi, Kohoku-ku, Yokohama 223, Japan

Received 31 October 1998; received in revised form 13 March 1999; accepted 23 March 1999

## Abstract

The structure of adsorbed bromine on the Ag(100) electrode has been studied with the in-situ XAFS (X-ray absorption fine structure) method. In the near edge XAFS (NEXAFS), the 1s–4p transition was clearly observed, which indicates that the electron transfer occurs from bromide anion to the silver substrate and the bond is partly covalent. The Br–Ag distance was determined to be  $2.82 \pm 0.05$  Å, which is shorter than that of the bulk AgBr. The adsorption site was revealed to be a fourfold hollow site. These results suggest that the bromide ionicity is reduced in the adsorbate phase on the electrode. © 1999 Elsevier Science S.A. All rights reserved.

**Keywords:** X-ray absorption fine structure (XAFS); Bromine; Silver; Adsorption

## 1. Introduction

Specific adsorption of halide ions on metal electrodes is one of the basic problems in interfacial electrochemistry. The study of the structure of adsorbate halogens is important because it plays crucial roles in electrochemical adsorption phenomena. In addition to ex-situ surface science techniques [1,2], recent in-situ techniques such as scanning tunnelling microscopy (STM) [3–7] and surface X-ray scattering (SXS) [8–17] have been devoted to revealing structures of adsorbed halogens on various single crystal electrode surfaces. However, both STM and SXS (and also ex-situ LEED) probe mostly the long-range ordering of the overlayer and give only a little information about important aspects of the interaction between adsorbate and substrate. In this aspect, in-situ X-ray absorption fine structure (XAFS) is an adequate tool, since it can provide the bond distance and the bonding properties between the adsorbate and substrate atoms.

Recently, Ocko et al. [13] investigated the system of bromine on silver(100) with SXS. It was revealed that in a 0.05 M NaBr solution, bromide ions start to adsorb on the silver(100) electrode at the potential of  $-1.2$  V (vs. Ag | AgCl). With a more positive potential, the coverage of bromine increases and the disorder–order phase transition occurs at  $-0.76$  V (0.35 ML). The ordered structure above the potential has a  $c(2 \times 2)$  overlayer. The coverage increases further up to 0.5 ml with the increase of potential to  $-0.5$  V. The adsorption site of bromine was determined to be a fourfold hollow site, in both the disordered and ordered phases. The distance between the  $c(2 \times 2)$  bromine and the substrate silver planes was reported to be 2.30 Å.

However, as described above, some aspects of the interaction between the bromine and silver atoms like the bond length and the bonding nature—either ionic or covalent—still remain unknown or are deduced only indirectly. Thus, we have applied the in-situ XAFS technique to the same system. In-situ Br K-edge XAFS measurements will provide us with direct information on these issues.

Since 1986, the in-situ XAFS technique has been adapted to the electrode | electrolyte interface mostly to

<sup>☆</sup> Presented at the International Symposium on Electrochemistry of Ordered Interfaces, Sapporo, Japan, 11–12 September, 1998.

\* Corresponding author.

E-mail address: ohta@chem.s.u-tokyo.ac.jp (T. Ohta)

investigate the structure of upd (deposited underpotentially) metals on silver, gold and platinum electrodes [18–29]. Most upd systems are complicated because there are at least two kinds of atoms – substrate and co-adsorbing anions – around the absorbing atom, and the overlayer is often incommensurate to the substrate. These factors make the EXAFS analysis difficult. In contrast, halogen atoms on a metal electrode undergo mono-adsorption (no coadsorbates except hydrating water) and seem to have a simpler structure. So we can take advantage of the XAFS method for this kind of system. To our knowledge, there have been no published results for in-situ XAFS studies of halogen atoms on metal electrodes.

From the experimental point of view, the system of bromide on a silver electrode has several advantages. Firstly, the energy of the bromine K absorption edge and that of the  $K\alpha$  fluorescence (ca. 13 keV) is in the region of hard X-rays that can transmit water with sufficient thickness. Secondly, silver as the substrate has no absorption edge in the bromine K-edge EXAFS energy region so that there is no kind of disturbing signal except scattered X-rays.

## 2. Experimental

Electrolyte solutions were prepared using high purity reagent (Wako pure chemical industries) and 18.3 MΩ cm Milli-Q water. In-situ XAFS experiments were performed in 50 μM NaBr solution. Such a low concentration was necessary for avoiding the signal from bromide ions in the bulk electrolyte solution. To enhance the conductivity, 0.05 M NaOH was added. The solution was bubbled with Ar gas to purge oxygen before the measurements. A silver single crystal of 10 mm diameter was purchased from Techno Chemicals and mechanically polished using alumina powder up to 0.05 μm. It was then etched chemically in a  $H_2O_2$  + sodium cyanide solution [30] just before the measurement and transferred into the cell protected by Milli-Q water. This procedure of the sample preparation was checked by cyclic voltammetry (CV) in a conventional electrochemical cell. We could obtain satisfactory CV curves similar to previous results [13] as shown in Fig. 1(a).

A specially designed electrochemical cell (Fig. 2) was used for in-situ XAFS experiments. The body of this cell was made of Teflon and polypropylene film of 6 μm thickness (Chemplex Industries) was used to protect the electrolyte solution from air exposure. The top of the cell was covered with an acrylic box (not shown in Fig. 2) with flowing nitrogen inside, in order to prevent oxygen migration into the electrolyte solution through the thin polypropylene window. The counter and the reference electrodes were Pt wires. All of this set were cleaned by heating in concentrated sulfuric acid before

the measurements. The reference potential of the Pt wire was adjusted to that of  $Ag|AgCl$  by the peak position of the CV in Fig. 1(a).

In the X-ray cell, it was impossible to obtain a CV like that in the conventional cell because the layer of solution between the working electrode and the other two electrodes was so narrow that the diffusion rate of ions was quite low. Therefore, the following procedure was done to check the sample condition. First, we took a CV in the conventional electrochemical cell which contained enough Br to ascertain the order-disorder transition peak. Then the electrode was taken out at the potential of the ordered phase ( $-0.35$  V vs.  $Ag|AgCl$ ), keeping the surface covered with water and transferred quickly into the X-ray cell at the same potential. It took a few seconds for this whole process. After all XAFS measurements (about 36 h), the sample was transferred back to the electrochemical cell and we measured the CV to check the Ag surface. The CV after the XAFS measurements showed almost the same features except for a small odd peak which might reflect slight surface roughening. Since the height of the odd peak was quite small, it might play a minor role in the present XAFS experiments.

In-situ XAFS measurements were performed at beamline 12C of the Photon Factory (photon energy of 2.5 GeV and stored ring current of 350–250 mA) in the Institute of Materials Structure Science, High Energy Accelerator Research Organization. This beamline consists of a Si(111) double crystal monochromator and a toroidal mirror to focus the monochromatized X-rays on the sample. Fig. 2 shows the experimental setup for in-situ Br K-edge XAFS measurements. The electro-

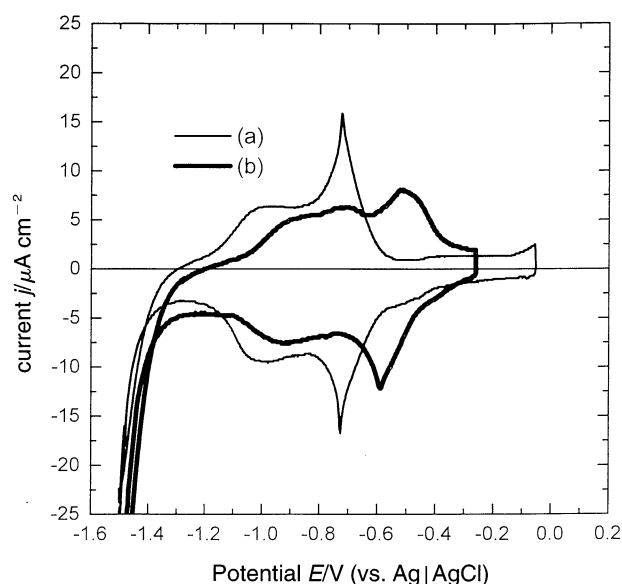


Fig. 1. Cyclic voltammogram of the Ag(100) electrode immersed in (a) 10 mM NaBr + 0.05 M NaOH, (b) 50 μM NaBr + 0.05 M NaOH. The scan rate is 10 mV s<sup>-1</sup>.

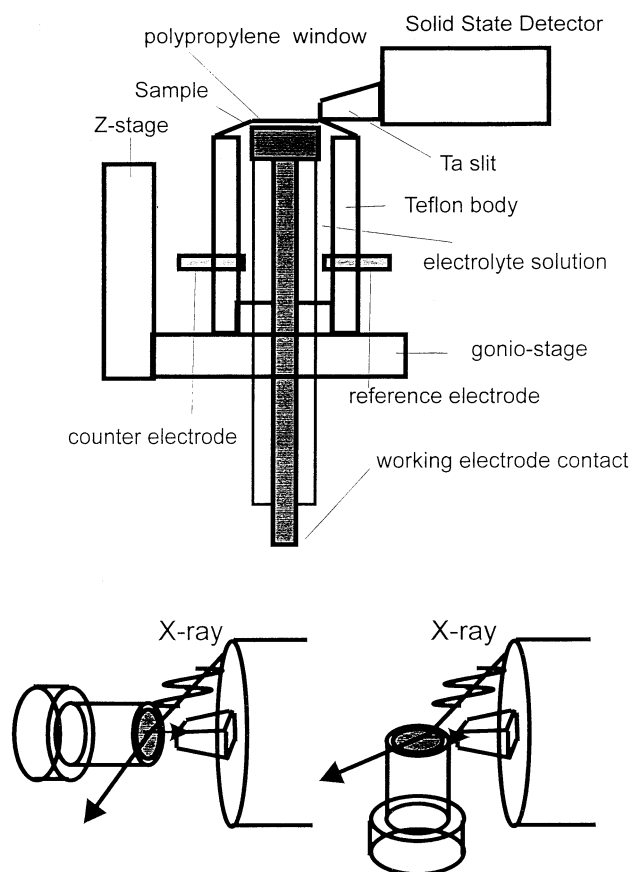


Fig. 2. Schematic drawing of the electrochemical cell designed specially for the XAFS measurements. Top: side view of setup for *s*-polarization. Bottom right: setup geometry for *s*-polarization. Bottom left: setup geometry for *p*-polarization.

chemical cell was mounted on *z*- and goniostages. In order to suppress the scattered X-rays, spectra were collected in the grazing-incidence (less than  $1^\circ$  of grazing angle) with the fluorescence X-ray detection mode. This grazing angle was attained by the pulse motor controlled adjustment of the *z*-movement and the rotation around the sample surface. *S*- and *p*-polarization measurements were performed by rotating the entire setup by  $90^\circ$ . Since the sample has only 10 mm diameter, the beam size at the sample was reduced by the XY slit to  $50\ \mu\text{m}$  height  $\times$  5 mm width at *s*-polarization, and 3 mm height  $\times$  100  $\mu\text{m}$  width at *p*-polarization measurement. A solid state detector which has an energy resolution of 150 eV at 13 keV was used to separate the signal fluorescence and the back ground scattered X-rays. A handmade Söller slit made of Ta was put in front of the solid state detector to minimize the scattered X-rays that come from the edge of the sample. The energy range of 13 300–13 900 eV was divided into three regions, pre-edge, NEXAFS, and EXAFS. The spectra were collected for 3, 5 and 10 s with energy steps of about 7, 1 and 5 eV for these respective regions in a single scan. More than 20 scans

were accumulated to obtain each spectrum. It took about 36 h for the total experiment. Fig. 3 shows the accumulated spectra of the in-situ EXAFS without any modification.

The spectra of solid silver bromide (powder) at 20 K and an aqueous bromide solution were obtained as references with the transmission mode.

### 3. Results and discussion

Fig. 1 shows a cyclic voltammogram of the Ag(100) electrode immersed in two solutions: (a) 10 mM bromide + 0.05 M NaOH and (b) 50  $\mu\text{M}$  bromide + 0.05 M NaOH. These CVs were taken in the conventional electrochemical cell. In solution (a), the order–disorder phase transition peak can be seen clearly at the potential of  $-0.75\ \text{V}$  in both the positive and negative scans as Ocko et al. indicated [13]. In solution (b), no distinguishable peak appeared in the positive scan because of the diffusion limit, but in the negative scan, the peak appeared at a potential shifted toward the positive side by 135 mV from that of solution (a). This peak potential movement obeys the Nernst equation. The peak appearance certainly suggests that the  $c(2 \times 2)$  ordered phase is formed above the peak potential even in such a low concentration solution. Br K-edge XAFS measurements were performed in 50  $\mu\text{M}$  bromide concentration and the electrode potential was held at  $-0.25\ \text{V}$  (vs. Ag | AgCl) to keep the  $c(2 \times 2)$  phase.

Fig. 4 shows the NEXAFS spectra of bromine on the silver(100) electrode together with some reference spectra. At the *s*-polarization experiment, the electric vector of incident X-rays is parallel to the surface and we can get information on surface-parallel unoccupied orbitals. On the other hand, for NEXAFS at *p*-polarization, the

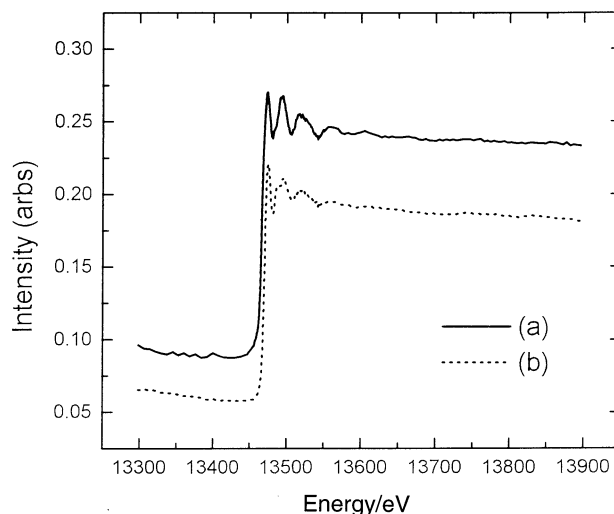


Fig. 3. The raw spectra of bromine on the Ag(100) electrode: (a) *p*-polarization and (b) *s*-polarization.

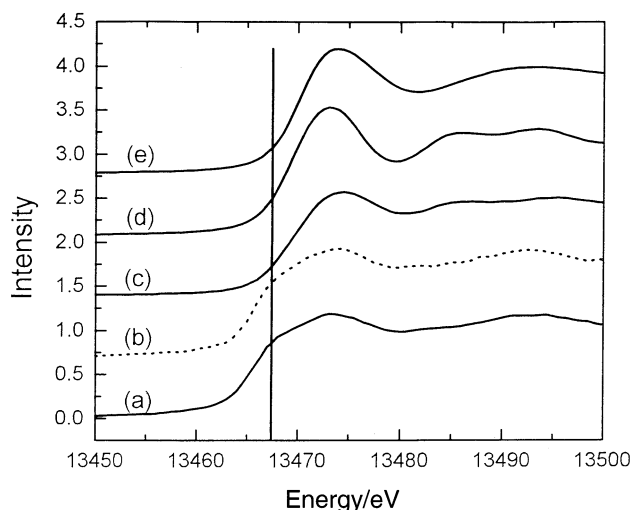


Fig. 4. The NEXAFS spectra of bromine on the Ag(100) electrode with some reference spectra. (a) The electrode potential is  $-0.25$  V (vs. Ag | AgCl),  $p$ -polarization. (b) The electrode potential is  $-0.45$  V (vs. Ag | AgCl),  $p$ -polarization. (c) The electrode potential is  $-0.25$  V (vs. Ag | AgCl),  $s$ -polarization. (d) Solid AgBr, measured with the transmission mode at 20 K (e) Bromide in aqueous solution, measured with the transmission mode at room temperature. The solid line indicates the shoulder position.

electric vector is normal to the surface and information on surface normal states can be obtained. Reference spectra are those of bulk AgBr and aqueous bromide ions.

There is a shoulder around the energy of 13 468 eV in the  $p$ -polarization spectra (a) and (b) which cannot be seen in either of the reference spectra. This shoulder can be assigned to the bromine  $1s \rightarrow 4p$  transition. The  $4p$  orbitals of the bromide in the bulk AgBr and the aqueous solution are fully occupied so that no  $1s \rightarrow 4p$  transition is expected in these two spectra. Qualitatively speaking, this result suggests that orbital hybridization between bromine and silver occurs and bromide loses its negative charge. The vacancy is found to be mainly in the  $p$  orbital directed along the surface normal, since there is no shoulder in the  $s$ -polarization spectrum (c). The quantitative analysis of NEXAFS would give us useful information about the electrosorption valency of the adsorbed bromine. Fig. 4 shows the spectrum at the electrode potential of  $-0.45$  V (vs. Ag | AgCl) at  $p$ -polarization, which has almost no difference from that of  $-0.25$  V. This means that potential (or coverage) dependence of the bromine electronic states in the  $c(2 \times 2)$  ordered phase is negligibly small.

EXAFS functions  $k^2\chi(k)$  ( $k$  is the wavenumber of photoelectrons) of bromine on silver (100) at  $-0.25$  V and their Fourier transforms are shown in Fig. 5. These functions were extracted from the raw spectra with the conventional procedure (background subtraction and normalization assuming the constant atomic absorption coefficient) [31]. Fourier transformed spectra show dou-

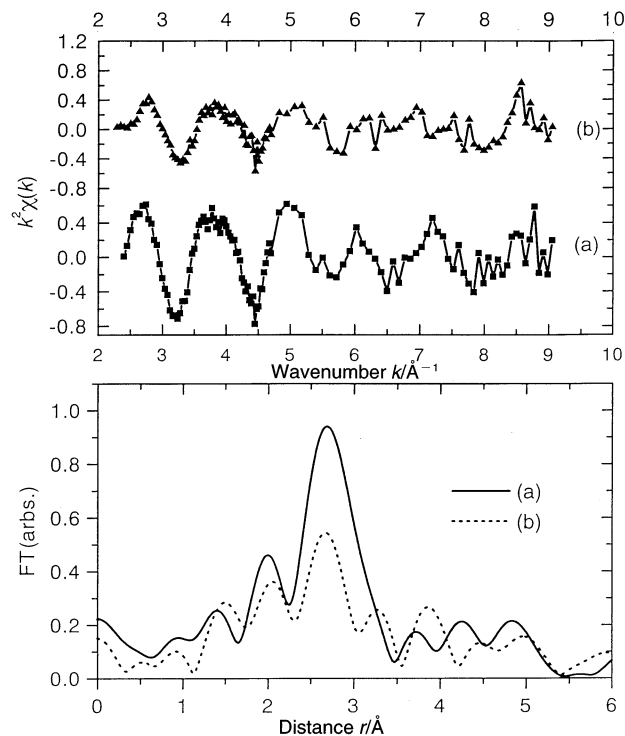


Fig. 5. Top: The EXAFS spectra of bromine on the Ag(100) electrode: (a)  $p$ -polarization and (b)  $s$ -polarization. Bottom: The Fourier transformations of the upper EXAFS spectra: (a)  $p$ -polarization and (b)  $s$ -polarization.

ble peaks between 1.7 and 3.4 Å, which are associated with the contribution of the nearest-neighbor Ag atoms. The peak splitting results from the Ramsauer–Townsend effect which causes double maxima in the backscattering amplitude for Ag. The curve-fitting analyses in  $k$  space were carried out after Fourier filtering of the peaks ( $\Delta r = 1.7 \sim 3.5$  Å for  $s$ -polarization and  $1.65 \sim 3.4$  Å for  $p$ -polarization) and subsequent inverse Fourier transformation. The spectrum of solid silver bromide at 20 K was used as a reference. The effective coordination number and the distance  $r(\text{Ag} - \text{Br})$  of the reference were assumed to be 6 and 2.86 Å, respectively. The energy correction  $\Delta E_0$ , the EXAFS Debye–Waller factor  $\sigma^2$  and the anharmonic correction term  $C_3$  were set to 0 so that these terms are represented as the relative values. The results of the analysis are summarized in Table 1. The parameters in parentheses were fixed during the curve fitting. The

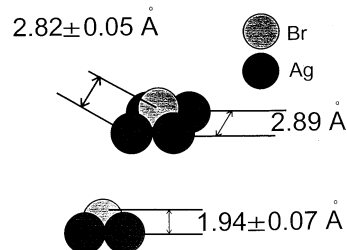


Fig. 6. Suggested structure model around the bromine atom on the Ag(100) electrode surface. Top: schematic view. Bottom: side view.

Table 1  
Results of the EXAFS analysis of the first-nearest neighbour Br–Ag shells<sup>a</sup>

Polarization	$N^*$	$r/\text{\AA}$	$\Delta E_0/\text{eV}$	$10^2 \sigma^2/\text{\AA}^2$	$10^3 C_3/\text{\AA}^3$	$R$
<i>s</i>	3.04	2.80	(2.84)	(0.87)	(0.88)	0.421
<i>p</i>	5.92	2.84	2.84	0.87	(0.88)	0.096

<sup>a</sup> The parameters in parentheses were fixed during the fitting.  $\Delta E_0$ ,  $\sigma^2$  and  $C_3$  are referred to those of bulk AgBr at 20 K. The coordination number  $N^*$  of AgBr ( $=6$ ) and  $\nu$  of AgBr ( $=2.86 \text{ \AA}$ ) were used as the reference.

$R$ -factor represents the goodness of fitting. It is known that the Br–Ag bond in bulk AgBr has large anharmonicity. The  $C_3$  value at 300 K was determined to be  $1.76 \times 10^{-3} \text{ \AA}^3$  referred to that at 20 K. On the other hand, there is no information available for the bond anharmonicity for adsorbed Br on the silver electrode. Thus, we assumed that  $C_3$  has the mean value of AgBr at 300–20 K ( $0.88 \times 10^{-3} \text{ \AA}^3$ ) in the analyses.

The bond length was determined as the mean value at *s*- and *p*-polarization:  $r = 2.82 \pm 0.05 \text{ \AA}$ . The bond distance  $r$  of bulk AgBr is  $2.89 \text{ \AA}$  at room temperature, while that of the diatomic molecule was found to be  $2.39 \text{ \AA}$  [32]. This means the covalent bond is shorter than the ionic bond. In this aspect, the shorter bond length of the adsorbate Br–Ag than that of bulk AgBr suggests the enhancement of covalency, which is consistent with the NEXAFS results indicating the partial charge transfer from bromine to the silver electrode.

The next issue is the adsorption site. The polarization dependence of the effective coordination number  $N^*$  provides information about the adsorption site. However, the absolute value of  $N^*$  contains inherent systematic errors. Thus, it is more reliable to compare the ratio of  $N^*$  at two polarizations (*s* and *p*) with that of the typical adsorption sites. These values are listed in Table 2. The experimental results conclude a 4-fold hollow site. A suggested structure model is given in Fig. 6.

The present results are in agreement with the SXS results [13] as far as the adsorption site is concerned, but the distances between bromine and silver are different from each other. Ocko et al. reported that the interplanar distance of the bromine and silver layer was  $2.30 \pm 0.3 \text{ \AA}$  (this error is the value as they noted for the Br/Au(111) system). Assuming the 4-fold hollow site adsorption, the interatomic distance  $r(\text{Br–Ag})$  amounts to  $3.08 \pm 0.2 \text{ \AA}$ , which is longer than our value.

Ignaczak and Gomes [33] performed ab initio calculations for the Br/Ag(100) cluster and obtained  $2.923 \text{ \AA}$  as the optimized Br–Ag distance. This is also longer than ours. About the adsorption site, the energy calculation by Ignaczak and Gomes [33] pre-

dicted the fourfold hollow site. This result is in agreement with ours.

Since these values seem to have relatively large errors, our results are not inconsistent with theirs. EXAFS has the advantage of determining the interatomic distance of the Br–Ag bond directly and more precisely.

Two processes in the sample preparation may cause some uncertainties in the results obtained: one is that the sample was free from the potential control for several seconds during the sample transfer from the CV cell to the X-ray cell. Silver bromide might be formed partially during this procedure. Another is that the sample surface might be oxidized during the EXAFS measurements, which took about 36 h. To check these effects, we measured CV just after the EXAFS measurements and ascertained that the sample surface was not changed significantly, although a small odd peak appeared which might come from roughed parts of the surface. Moreover, the Br K-edge EXAFS clearly indicated that the Br atoms are surrounded mostly by Ag atoms. The absolute coordination numbers obtained in our experiment (see Table 1) are in good agreement with those of calculated ones (5.6 for *p*-polarization and 3.15 for *s*-polarization). If the electrode surface were significantly oxidized and Br atoms were on the oxide surface, too, the experimental coordination number for the Br–Ag bond would become much smaller. This means that even if there were a certain amount of silver oxide on the surface, Br atoms would be adsorbed only on a clean Ag surface. This causes only the decrease of the Br atomic population on the electrode. Since what we observed is the region where Br is adsorbed, oxide parts do not affect the local structure of Br on Ag. In order to reduce the ambiguity of the EXAFS analysis, a new X-ray cell is now under design, which makes in-situ CV measurements possible.

Table 2  
The ratio of the effective coordination numbers of two polarizations

Calculated	Experimental		
	4-Fold hollow	Bridge	Atop
0.553	0.178	0.0	0.514

#### 4. Conclusions

In-situ XAFS of the adsorbed bromine on the silver(100) electrode for the  $c(2 \times 2)$  phase was measured. The results are as follows:

(1) The distance between the bromine and the silver atom is  $2.82 \pm 0.05$  Å. This value is longer than that of diatomic AgBr (2.39 Å), and is shorter than that of the ionic compound AgBr (2.89 Å).

(2) There is charge transfer from adsorbate bromide to substrate silver, although the quantitative analysis is not yet performed.

(3) The bromine–silver bond is more ionic than that of diatomic AgBr, but more covalent than that of bulk AgBr.

#### Acknowledgements

We are grateful for the financial support of the Grant-in-Aid for Scientific Research (No.10131214). The present work has been performed under the approval of the Photon Factory Program Advisory Committee (PF-PAC No.97G047).

#### References

- [1] G.N. Salaita, F. Lu, L.L.- Davidson, A.T. Hubbard, J. Electroanal. Chem. 229 (1987) 1.
- [2] M.S. Zei, J. Electroanal. Chem. 308 (1991) 295.
- [3] X. Gao, M.J. Weaver, J. Am. Chem. Soc. 114 (1992) 8544.
- [4] G. Aloisi, A.M. Funtikov, T. Will, J. Electroanal. Chem. 370 (1994) 297.
- [5] M.L. Foresti, G. Aloisi, M. Innocenti, H. Kobayashi, R. Guidelli, Surf. Sci. 335 (1995) 241.
- [6] T. Teshima, K. Ogaki, K. Itaya, J. Phys. Chem. 101 (1997) 2046.
- [7] T. Yamada, N. Batina, K. Itaya, J. Phys. Chem. 99 (1995) 8817.
- [8] B.M. Ocko, G.M. Watson, J. Wang, J. Phys. Chem. 98 (1994) 897.
- [9] O.M. Magnussen, B.M. Ocko, R.R. Adžić, J.X. Wang, Phys. Rev. B 51 (1995) 5510.
- [10] B.M. Ocko, O.M. Magnussen, J.X. Wang, R.R. Adžić, T. Wandlowski, Physica B 221 (1996) 238.
- [11] O.M. Magnussen, B.M. Ocko, J.X. Wang, R.R. Adžić, J. Phys. Chem. 100 (1996) 5500.
- [12] J.X. Wang, G.M. Watson, B.M. Ocko, J. Phys. Chem. 100 (1996) 6672.
- [13] B.M. Ocko, J. Wang, T. Wandlowski, Phys. Rev. Lett. 79 (1997) 1511.
- [14] C.A. Lucas, N.M. Marković, P.N. Ross, Surf. Sci. 340 (1995) L949.
- [15] C.A. Lucas, N.M. Marković, I.M. Tidswell, P.N. Ross, Physica B 221 (1996) 245.
- [16] N.M. Marković, C.A. Lucas, H.A. Gasteiger, P.N. Ross, Surf. Sci. 365 (1996) 229.
- [17] C.A. Lucas, N.M. Marković, P.N. Ross, Phys. Rev. B 55 (1997) 7964.
- [18] L. Blum, H.D. Abruña, J. White, J.G. Gordon II, G.L. Borges, M.G. Samant, O.R. Melroy, J. Chem. Phys. 85 (1986) 6732.
- [19] O.R. Melroy, M.G. Samant, G.L. Borges, J.G. Gordon II, L. Blum, J.H. White, M.J. Albarelli, M. McMillan, H.D. Abruña, Langmuir 4 (1988) 798.
- [20] J.H. White, H.D. Abruña, J. Electroanal. Chem. 274 (1989) 185.
- [21] H.S. Yee, H.D. Abruña, J. Phys. Chem. 97 (1993) 6278.
- [22] H.S. Yee, H.D. Abruña, Langmuir 9 (1993) 2460.
- [23] G.M. Bommarito, D. Acevedo, J.F. Rodriguez, H.D. Abruña, J. Electroanal. Chem. 379 (1994) 135.
- [24] M.G. Samant, G.L. Borges, J.G. Gordon II, O.R. Melroy, L. Blum, J. Am. Chem. Soc. 109 (1987) 5970.
- [25] G. Tourillon, D. Guay, A. Tadjeddine, J. Electroanal. Chem. 289 (1990) 263.
- [26] A. Tadjeddine, D. Guay, M. Ladouceur, G. Tourillon, Phys. Rev. Lett. 66 (1991) 2235.
- [27] R. Durand, R. Faure, D. Aberdan, C. Salem, G. Tourillon, D. Guay, M. Ladouceur, Electrochim. Acta 41 (1996) 1947.
- [28] T.E. Furtak, L. Wang, J. Pant, K. Pansewicz, T.M. Hayes, J. Electrochem. Soc. 141 (1994) 2369.
- [29] S. Wu, Z. Shi, J. Lipkowski, A.P. Hitchcock, T. Tyliszczak, J. Phys. Chem. B 101 (1997) 10310.
- [30] J.N. Jovićević, V.D. Jović, A.R. Despić, Electrochim. Acta. 29 (1984) 1625.
- [31] See, for instance, D.C. Koningsberger, R. Prins. X-ray Absorption: Principles, Applications, Techniques of EXAFS, SEXAFS and XANES, Wiley, NY, 1988.
- [32] The Chemical Society of Japan, Kagaku-Binran, Maruzen, 1993.
- [33] A. Ignaczak and J.A.N.F. Gomes. J. Electroanal. Chem., 420 (1997) 71.